Experimental determination of frequency response function estimates for flexible joint industrial manipulators with serial kinematics

Florian Saupe and Andreas Knoblach

Citation Notice

[1] Florian Saupe and Andreas Knoblach. Experimental determination of frequency response function estimates for flexible joint industrial manipulators with serial kinematics. *Mechanical Systems and Signal Processing*, 52–53:60–72, 2015. doi:10.1016/j.ymssp.2014.08.011.

```
@ARTICLE{Saupe2015,
  title                = {Experimental determination of frequency response function estimates for flexible joint industrial manipulators with serial kinematics},
  author               = {Florian Saupe and Andreas Knoblach},
  journal              = {Mechanical Systems and Signal Processing},
  year                 = {2015},
  pages                = {60--72},
  volume               = {52--53},
  doi                  = {10.1016/j.ymssp.2014.08.011},
}
```

Experimental Determination of Frequency Response Function Estimates for Flexible Joint Industrial Manipulators with Serial Kinematics

Florian Saupe[a], Andreas Knoblach[a,*]

[a] *German Aerospace Center, Robotics and Mechatronics Center, Institute of System Dynamics and Control, Münchner Straße 20, 82234 Weßling, Tel.: +49 8153 28-1381, Fax: +49 8153-28 1441*

Abstract

Two different approaches for the determination of frequency response functions (FRFs) are used for the non-parametric closed loop identification of a flexible joint industrial manipulator with serial kinematics. The two applied experiment designs are based on low power multisine and high power chirp excitations. The main challenge is to eliminate disturbances of the FRF estimates caused by the numerous nonlinearities of the robot. For the experiment design based on chirp excitations, a simple iterative procedure is proposed which allows exploiting the good crest factor of chirp signals in a closed loop setup. An interesting synergy of the two approaches, beyond validation purposes, is pointed out.

Keywords: Frequency Response Function, Closed Loop Identification, Experiment Design, Flexible Joint Manipulator, Multisine, Chirp

1. Introduction

This paper focuses on closed loop experiment designs for the estimation of frequency response functions (FRFs) of flexible joint industrial manipulators with serial kinematics.[1] The considered standard six axis robot is depicted in Figure 1. The experimentally determined FRF estimates are eventually used in the feedback controller design for the manipulator. While most nonlinearities are compensated by a feedforward controller, the aim of the feedback controller is to ensure stationary accuracy and to improve the disturbance rejection. While the former aim can be easily fulfilled by an integrating controller, the latter one requires accurate models in the mid frequency range. This frequency range is governed by the robot's elasticities and characterized by distinct resonances and antiresonances in the FRFs. Note that although the overall robot dynamics is nonlinear, the dynamics of interest can be well described by linear models – at least in the neighborhood of a fixed operating point. However, existing nonlinearities can greatly disturb experimentally determined FRFs. The difficult choice of excitation signals w. r. t. a minimization of the disturbing impact of nonlinearities like Coulomb friction is the subject of this paper.

Even though frequency domain approaches for the identification of industrial robots are common, see e. g. [5, 1, 3], the choice of excitation signals is often neglected. In [5], plain multisine and chirp excitations are applied without additional measures to avoid or even estimate the impact of the acting nonlinearities. A friction compensation is applied in [1]. The approach of [3] resorts to an open loop identification in order to guarantee a strong excitation of the robot. The strong excitation is expected to render the influence of Coulomb friction negligible. A hybrid identification, i. e. a mix of frequency domain and time domain methodology, is proposed in [7]. Frequency domain methods are used to identify the model parameters corresponding to the elasticities. In order to avoid disturbances due to Coulomb friction, the zero velocity regime is avoided by superimposing a multisine excitation with a constant velocity profile. The impact of nonlinearities on the FRF estimates obtained with multisine excitations is studied in

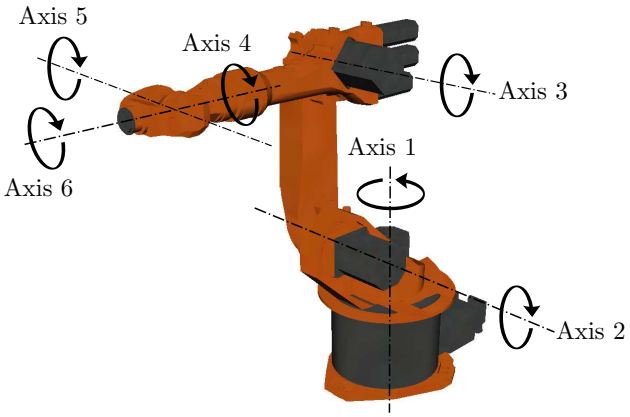

Figure 1: A standard six axis industrial manipulator.

*Corresponding author
Email address: Andreas.Knoblach@dlr.de (Andreas Knoblach)

[1] The words *manipulator* and *robot* refer always to flexible joint industrial manipulators with serial kinematics in the remainder of the paper.

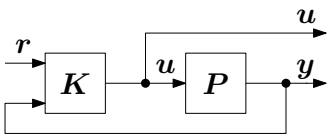

Figure 2: A closed loop identification scenario.

[8]. The present paper extends these insights and considers chirp excitations as an alternative. Note that the proposed approaches can be used for a wide class of positioning machines, as long as a linear model around a working point can be reasonably defined.

In Section 2, the challenges of experiment designs for the identification of industrial robots are captured. Some basics on the estimation of FRFs are given in Section 3. Possibilities to tackle the challenges of the experiment design for each of the two approaches are discussed in the Sections 4 and 5. A procedure which allows to purposefully choose closed loop excitation signals is proposed in Section 5.3. An academic example given in Section 6 serves as an illustration. Finally, the FRF estimates obtained from hardware testbed experiments with the considered industrial robot are analyzed and compared in Section 7.

2. Challenges for the Experiment Design

Since the open loop of a serial kinematics robot is an unstable system, a closed loop identification is performed. See Figure 2 for a typical closed loop configuration with a controller $\boldsymbol{K}$ and the plant $\boldsymbol{P}$, of which the FRF estimate is to be determined. The measurement vector is $\boldsymbol{y} \in \mathbb{R}^{n_y}$, the input vector is $\boldsymbol{u} \in \mathbb{R}^{n_u}$ and the vector of reference signals is $\boldsymbol{r}$. Without loss of generality, it is assumed that $\boldsymbol{r} \in \mathbb{R}^{n_u}$. It is usually preferred to insert the excitation as a reference signal for the controller instead of a disturbance in the input of the plant. However, since an experimental controller is used, the excitation signal is not well tracked, i. e. $\boldsymbol{y} \neq \boldsymbol{r}$.

A serial kinematics robot is subject to many nonlinearities. Some of these nonlinearities result in major disturbances of the FRF estimate and appropriate measures must be taken to lessen or eliminate these disturbances. Other nonlinearities lead to restrictions on the choice of excitation signals. They all must be considered as early as possible in the experiment design.

A Dynamic gear load constraints:
In order to prevent an overburdening of the transmission risking a mechanical failure, the dynamic gear load of the robot must be limited. For most robot systems, the crucial states for a determination of the dynamic gear load are not available as measurements. As a remedy, another informative signal which determines the dynamic gear load must be limited. It is proposed to use the commanded motor torque $\boldsymbol{\tau}_m$, i. e. the plant input $\boldsymbol{u}$, as a guide value for the gear load. Note that there are also link load constraints. However, for the considered robot, they are far beyond the gear load limits. The link loads are consequently neglected below.

B Coulomb friction:
Perhaps the most problematic nonlinearity is Coulomb friction which introduces severe disturbances for velocities around zero. Coulomb friction opposes motion with a friction torque of velocity independent amplitude. With the velocity $\dot{q}$, Coulomb friction can be modeled as

$$\tau_{f,c}(\dot{q}) = F_c \operatorname{sgn}(\dot{q}) . \tag{1}$$

If the excitation of the considered system is not strong enough[2] or the low velocity regime is not avoided, nonlinear friction tends to conceal the resonances and antiresonances in the FRF estimate by acting as a strong damping force.

C Nonlinear deflection dependent stiffness:
The deflection of the spring damper combination modeling the transmission varies with different excitations. The following nonlinear spring torque is considered in e. g. [7]. With the deflection between the motor and link position $\Delta q = q_m - q_o$, the stiffness coefficients k_1 and k_2, and the deflection b_s at which the slope of the stiffness characteristic switches from k_1 to k_2 (usually, $k_2 > k_1$), the nonlinear spring torque is given by

$$\tau_{s,d}(\Delta q) = \begin{cases} k_1 \Delta q & |\Delta q| \leq b_s, \\ \operatorname{sgn}(\Delta q)\,(k_2(|\Delta q| - b_s) + k_1 b_s) & |\Delta q| > b_s. \end{cases} \tag{2}$$

If the stiffness characteristic is deflection dependent, the FRF estimate obtained from an experiment also varies for different excitations. Consequently, the peaks of the characteristic resonances and antiresonances shift in dependency of the chosen excitation. It is not the aim of this paper to find the optimal way how a deflection dependent stiffness can be represented in an FRF estimate. The goal is simply to detect its presence.

D Position dependent dynamics:
The mass distribution of the robot depends on the individual axis positions. Large deviations from the initial position should be avoided during an experiment. It is decided to allow a maximum deviation of about $\pm 4°$ per axis in the identification experiments.

E Periodic disturbances:
The permanent magnet synchronous motors of the considered robot generate torque ripples which act as

[2] A harmonic excitation is referred to as strong enough if the root mean square value of the resulting motor torque is well above F_c.

periodic disturbances, see [4]. Especially for low velocities, the resulting disturbances become severe. Note that there might be further periodic disturbances for other types of motors and/or transmissions.

F Measurement and discretization noise: Most industrial robots only provide motor position measurements. Even though the resolution of the position increments is often extremely high, there is severe noise in the velocity signals obtained by numerical differentiation. This noise is fed back in a closed loop setting. The motors themselves also introduce noise as the servo electronics can only command the current, i. e. the motor torque, on an incremental basis.

G Coriolis and gravity forces: Since the robot is not allowed to move by more than $\pm 4°$ per axis from the operating point that is to be identified, there are no high velocities. The resulting Coriolis forces have no impact on the dynamics. Due to the quasi static position, the gravity torques act like constant disturbances with no impact on the dynamics.

3. Estimation of Frequency Response Functions

The goal of this section is to determine non-parametric estimates of an FRF giving the relationship between the input vector $\boldsymbol{u}$ and the output vector $\boldsymbol{y}$ in the frequency domain. The continuous signals are sampled with the sample time T_s. Using $t_i = iT_s$, the sampled $\boldsymbol{u}$ with n_f samples is given by $\boldsymbol{u}(t_i) \in \mathbb{R}^{n_u}$, $i \in \{0, \ldots, n_f - 1\}$. The sampled signals are transformed into the frequency domain via discrete Fourier transforms (DFTs) of length n_f, e. g.

$$\boldsymbol{u}(t_i) \overset{\text{DFT}}{\underset{n_f}{\longmapsto}} \boldsymbol{U}(\omega_k) \tag{3}$$

with $\boldsymbol{U}(\omega_k) \in \mathbb{C}^{n_u}$ and the normalized frequencies $\omega_k = k\frac{2\pi}{n_f}$, $k = 0, \ldots, n_f$.

Remark 1 (Normalized frequencies ω_k)**.** *If a DFT is applied to a real signal $\boldsymbol{u}(t_i)$, the resulting $\boldsymbol{U}(\omega_k)$ is symmetric s. t. $\boldsymbol{U}(\omega_{n_f-k}) = \operatorname{conj}(\boldsymbol{U}(\omega_k))$. The normalized, dimensionless frequencies ω_k with $k \leq n_f/2$ correspond to the frequencies $f_k = \frac{k}{T_s n_f}$.*

In the mapping

$$\boldsymbol{Y}(\omega_k) = \boldsymbol{P}(\omega_k)\boldsymbol{U}(\omega_k), \tag{4}$$

the term denoted $\boldsymbol{P}(\omega_k) \in \mathbb{C}^{n_y \times n_u}$ is the FRF. In order to obtain an FRF estimate $\hat{\boldsymbol{P}}(\omega_k)$ of a plant, it is excited with different realizations of input signals, i. e. with $\boldsymbol{U}_s(\omega_s) \in \mathbb{C}^{n_u}$, $s \in \{1, \ldots, n_{ex}\}$ in $n_{ex} \geq n_u$ experiments. The $\boldsymbol{U}_s(\omega_k)$ are stored in a matrix $\mathbb{U}(\omega_k) \in \mathbb{C}^{n_u \times n_{ex}}$ of the form

$$\mathbb{U}(\omega_k) = \begin{bmatrix} \boldsymbol{U}_1(\omega_k) & \cdots & \boldsymbol{U}_{n_{ex}}(\omega_k) \end{bmatrix}. \tag{5}$$

The corresponding responses of the system

$$\boldsymbol{Y}_s(\omega_k) \in \mathbb{C}^{n_y}, s \in \{1, \ldots, n_{ex}\} \tag{6}$$

are analogously stored in a matrix $\mathbb{Y}(\omega_k)$. The FRF estimate $\hat{\boldsymbol{P}}(\omega_k)$ can be calculated as

$$\hat{\boldsymbol{P}}(\omega_k) = \mathbb{Y}(\omega_k)\mathbb{U}(\omega_k)^{\dagger}. \tag{7}$$

In the latter expression, $\mathbb{U}(\omega_k)^{\dagger}$ denotes the pseudo inverse of $\mathbb{U}(\omega_k)$. In order to obtain good results using (7), $\mathbb{U}(\omega_k)$ should have full row rank.

4. Odd Random Multisine Excitations

Odd random multisine excitation signals are proposed in [6] for the identification of nonlinear systems. This kind of excitation has already been adapted in [7] for the identification of industrial manipulators. A scalar random multisine signal is a broadband signal of the form

$$r_{\text{ms}}(t, \phi) = \sum_{s=1}^{n_s} A_s \sin(2\pi f_s t + \phi_{\text{rand},s} + \phi). \tag{8}$$

The frequencies f_s with $s \in \{1, \ldots, n_s\}$ are integer multiples of a fundamental frequency f_0. A multisine (8) is referred to as odd if only odd multiples of f_0 are considered. The multisine is referred to as random if random phases $\phi_{\text{rand},s}$ are chosen s. t. the expected mean value over all s is $\mathrm{E}(e^{\mathrm{j}\phi_{\text{rand},s}}) = 0$. The extra argument ϕ allows to alter the phase of the excitation in the individual channels of a MIMO excitation.

Due to the broadband characteristic of a multisine signal, its signal to noise ratio is low. Its crest factor, i. e. the ratio between the maximum power at any point in time to the mean power over the experiment is high, see [2].

As of now, the terms multisine and random multisine will always refer to odd random phase multisines.

4.1. Definition of an Excitation Signal for MIMO Experiments

For MIMO identification, orthogonal random multisine excitations are proposed in [7]. A number of $n_{ex} = n_u$ experiments are performed. The phases of the excitation (8) are shifted by $\phi_{l,m} = \frac{2\pi}{n_u}(l-1)(m-1)$ for different channels (index l) and experiments (index m). The resulting MIMO excitation is captured in the matrix

$$\mathbb{R}_{\perp}(\omega_k) \overset{\text{DFT}}{\underset{n_f}{\longmapsto}} \mathbb{r}_{\perp}(t_i) = \begin{bmatrix} r_{\text{ms}}(t_i, \phi_{1,1}) & \cdots & r_{\text{ms}}(t_i, \phi_{1,n_{ex}}) \\ \vdots & \ddots & \vdots \\ r_{\text{ms}}(t_i, \phi_{n_u,1}) & \cdots & r_{\text{ms}}(t_i, \phi_{n_u,n_{ex}}) \end{bmatrix}. \tag{9}$$

As in (5), the i^{th} column of $\mathbb{R}_{\perp}(\omega_k) \in \mathbb{C}^{n_u \times n_{ex}}$ collects the data of the i^{th} MIMO experiment. Due to the phase shifts, this approach yields an $\mathbb{R}_{\perp}(\omega_k)$ with the optimal condition number 1.

4.2. Signal Design and Signal Processing

The amplitudes A_s of the individual sine components in the multisine excitation (8) are usually chosen s. t. the resulting signal does not exceed a predefined threshold. The frequencies f_s with $s \in \{1, \ldots, n_s\}$ of the individual sine components are chosen such that they correspond to the normalized frequencies of the DFT which is used to transform the signals into the frequency domain. This allows to avoid the leakage effect which disturbs the results of a DFT if a non periodic signal is analyzed. But as a consequence, the signal design and signal processing are highly involved.

In practice, a lower and an upper bound for the frequencies in the excitation are chosen, $\tilde{f}_l$ and $\tilde{f}_u$. The frequencies f_s with $s \in \{1, \ldots, n_s\}$ should correspond to a set of about 80 roughly logarithmic distributed frequencies with $f_1 \approx \tilde{f}_l$ and $f_{n_s} \approx \tilde{f}_u$ such that the frequency resolution of the resulting FRF estimate is good. A set with exactly 80 logarithmically distributed frequencies in $[\tilde{f}_l, \tilde{f}_u]$ is denoted $\tilde{\boldsymbol{F}}$ and will be used as a reference. In order to make sure that the frequencies f_s with $s \in \{1, \ldots, n_s\}$ also coincide with the normalized frequencies of the DFT, the signal processing must be considered. In the signal processing, the original data has its average subtracted from it. Afterward, it is resampled s. t. the new sample time is

$$T_s \approx \frac{5}{\tilde{f}_u}. \tag{10}$$

The new sample time T_s determines the highest frequency resolved by the DFT. The frequency resolution of the DFT can be adjusted by varying the number of samples by appending zeros to the data series.[3] The resulting number of total samples is denoted n_f. With n_f and T_s, the frequency resolution of the DFT is

$$f_0 = \frac{1}{T_s n_f}. \tag{11}$$

It is used as the fundamental frequency f_0 of the multisine signal, hence the use of the corresponding symbol. The fundamental frequency f_0 thus determines the minimum distance between two frequencies f_s in the spectrum of the multisine. Since the excitation must last an exact integer multiple of f_0 to avoid leakage effects, f_0 also determines the duration of the experiment. If f_0 is too low, the duration of the experiment becomes overly long. If f_0 is too high, the achievable frequency resolution is poor. With a desired maximum frequency resolution $\tilde{f}_0$, the required n_f can be chosen based on (11) s. t.

$$n_f = \operatorname{ceil}\left(\frac{1}{\tilde{f}_0 T_s}\right). \tag{12}$$

Finally, the frequencies f_s with $s \in \{1, \ldots, n_s\}$ are chosen as the odd multiples of f_0 which are nearest to the elements of the desired frequency set $\tilde{\boldsymbol{F}}$.

[3] In such a zero padding, the number of zeros is chosen s. t. the resulting n_f is a power of 2. This allows to apply the effective fast Fourier transformation algorithm.

4.3. Calculating a Best Linear Approximation

In [6], a best linear approximation $\hat{\boldsymbol{P}}_l(\mathrm{j}\omega)$ of so called Volterra systems[4] is obtained based on experiments with odd random multisine excitations. The theory will not be established in this paper. The interested reader is referred to [6]. According to the theory, the response of the considered class of systems can be written as

$$\boldsymbol{P}(\omega_k) = \hat{\boldsymbol{P}}_l(\omega_k) + \boldsymbol{P}_{nl}(\omega_k) + \boldsymbol{N}(\omega_k) \tag{13}$$

with the best linear approximation $\hat{\boldsymbol{P}}_l(\omega_k)$ of the nonlinear system, a zero mean stochastic nonlinear contribution $\boldsymbol{P}_{nl}(\omega_k)$ and the measurement noise $\boldsymbol{N}(\omega_k)$. For any fixed excitation, the nonlinear contribution $\boldsymbol{P}_{nl}(\omega_k)$ is deterministic. With the number of harmonics n_s sufficiently high and different (random) realizations of multisine excitation signals, $\boldsymbol{P}_{nl}(\omega_k)$ acts like circular complex noise. In order to determine $\hat{\boldsymbol{P}}_l(\omega_k)$, it is possible to subsequently eliminate the impact of the measurement noise and the nonlinearities by performing an averaging. It is noted that while the random property of the multisine is essential for the theory of a best linear approximation, the odd property simply helps to average out the nonlinearities more quickly, see [6].

A number of n_p different realizations of the multisine excitation (9), i. e. with different random phases $\phi_{\mathrm{rand},s}$, are calculated. Each of these realizations of the excitation is applied n_q times. From the collected data, a family of $n_p \times n_q$ FRF estimates $\hat{\boldsymbol{P}}^{[p,q]}(\omega_k)$ is obtained with $p \in \{1, \ldots, n_p\}$ (index corresponding to the different realizations) and $q \in \{1, \ldots, n_q\}$ (index corresponding to the repetition of the same realization). By averaging over the results corresponding to the n_q applications of the same realization of the excitation, the influence of measurement noise can be eliminated. Averaging over the n_p different realizations of the excitation allows to eliminate the stochastic nonlinear contribution and finally leads to $\hat{\boldsymbol{P}}_l(\omega_k)$. In this paper, the simple arithmetic mean estimator is used for the averaging s. t.

$$\hat{\boldsymbol{P}}_l(\omega_k) = \frac{1}{n_p n_q} \sum_{p=1}^{n_p} \sum_{q=1}^{n_q} \hat{\boldsymbol{P}}^{[p,q]}(\omega_k). \tag{14}$$

For a comparison of different methods for the estimation of FRFs from experimental data, the reader is referred to [9].

4.4. Answers to the Challenges: Multisine Experiment

In this section, answers to the challenges stated in Section 2 are provided for experiments based on odd random multisine excitations. The necessary individual measures are conflicting. It is thus imperative to carefully choose a compromise based on some understanding of the system which is to be identified.

[4] A Volterra system is a certain kind of nonlinear system. In principle, it is comparable to a Taylor series but with the capability to cover memory effects. See [6] for details.

A Dynamic gear load constraints:
The maximum amplitude of the excitation signal must be limited to a reasonable value. Due to the bad crest factor of multisine signals, this leads to relative weak average excitations.

B Coulomb friction:
Due to the weak excitation of the system, the best linear approximation FRF estimate calculated from a plain multisine excitation is greatly influenced by Coulomb friction. The superposition of the excitation signal with a constant velocity in order to avoid the zero velocity regime as proposed in e. g. [7] allows to eliminate the impact of Coulomb friction.

C Nonlinear deflection dependent stiffness:
The effects of nonlinear deflection dependent stiffness may be regarded as a nonlinear contribution which can be eliminated by averaging if a reasonable number of different random realizations of multisine excitations is used. However, since the overall amplitude of the excitation signal is limited (according to the arguments in the preceding items) and the static load can be small or even zero (e. g. for the axis 1), it cannot be ensured that the resulting spring torques are strong enough to trigger the nonlinear characteristic of the stiffness.

D Position dependent dynamics:
The maximum allowed position deviation per axis has an impact on the maximum constant velocity profile that may be superimposed with the excitation in order to avoid zero velocities.

E Periodic disturbances:
A constant velocity profile superimposed on the excitation signal may lead to severe periodic disturbances. The following remedy is proposed. By performing an experiment with the constant velocity profile but without the multisine excitation, the deterministic periodic disturbances can be recorded. The data collected in the experiments with multisine excitations can be corrected using the information gained in the additional experiment. The time series of the experiment without multisine excitation is simply subtracted from the time series of the experiment with multisine excitation. A further, if rather insignificant advantage is that the slowly time varying bias of the plant input due to a varying gravity force is also eliminated.[5]

F Measurement and discretization noise:
The limited maximum amplitude of the excitation in combination with its bad crest factor makes multisine experiments sensitive to noise. The influence of noise may be reduced by averaging over several experiments at the cost of a longer overall identification procedure.

[5]The gravity torques vary slightly due to the deviation from the initial position.

5. Chirp Excitations

According to [2], chirp excitations are sinusoids with a frequency $f(t)$ that changes continuously over a band $[f_l, f_u]$ over a time interval $[t_0, t_1]$. The phase ϕ is introduced as an additional parameter in the chirp signal in order to allow for phase shifts between excitations in a MIMO experiment. With the time dependent amplitude[6] $A(t)$, a chirp signal is given by

$$r_c(t, \phi) = A(t) \sin\left(2\pi \int_{t_0}^{t} f(\tau)\mathrm{d}\tau + \phi\right), t \in [t_0, t_1]. \quad (15)$$

The frequencies are chosen s. t. they depend exponentially on time as in

$$f(t) = \mathrm{e}^{a_0 t + a_1}. \quad (16)$$

The constants a_0 and a_1 are determined by a choice of $f(t_0) = f_l$ and $f(t_1) = f_u$. The excitation signal (15) is harmonic and emphasizes low frequencies.

The signal to noise ratio of chirp excitations is very good. Its crest factor (i. e. the ratio between the maximum power at any point in time to the mean power over the experiment) is good.

In analogy to (9), MIMO experiments can be performed by shifting the phases of the excitation signals between the channels of the excitation signals and the individual experiments. A suitable MIMO chirp excitation signal is obtained by using (9), replacing all multisine signals r_{ms} by chirp signals r_c.

There are no results on best linear approximations obtained from experiments based on chirp excitations. Appropriate measures to avoid distortions of the FRF estimate are proposed in the subsequent sections.

5.1. Signal Design and Signal Processing

The time depending amplitude of the chirp excitation (15) is chosen s. t. it is below a predefined threshold. In combination with a choice of the frequency band $[f_l, f_u]$ and a duration $t_1 - t_0$, a suitable chirp signal is defined. The coordination of the signal design and the signal processing for chirp excitations is not as involved as it is for multisine excitations, since all frequencies in the band $[f_l, f_u]$ are excited. However, higher harmonics (see Figure 3) might deteriorate the FRF estimates. A thorough signal processing allows to minimize such effects and the following procedure is proposed.

The set of frequencies for which the FRF estimate is calculated, e. g. a logarithmically distributed set $\tilde{\boldsymbol{F}}$, is defined in the signal processing step. This set of frequencies must be a subset of the frequency band $[f_l, f_u]$. From (16), it is known exactly which frequency is excited at which time. With that knowledge, it is possible to analyze only

[6]It is assumed that the amplitude varies slowly compared to the frequency f_l.

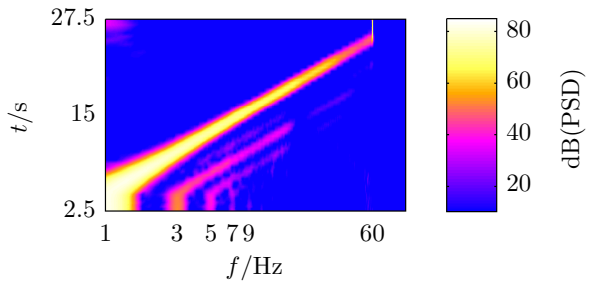

Figure 3: Power spectral density (PSD) over time of the axis 3 motor torque during a chirp excitation.

an excerpt of the chirp signal for each frequency $f_x \in \tilde{\boldsymbol{F}}$. The results in this paper are based on the evaluation of four periods of the considered frequencies. Each excerpt, which corresponds to a certain frequency f_x, has its mean value subtracted from it. Afterwards, the data is filtered, down sampled to about ten samples per period of f_x and a Hann window is applied before the DFT is calculated.

5.2. Answers to the Challenges: Chirp Experiment

In this section, answers to the challenges stated in Section 2 are provided for experiments based on chirp excitations. Due to the very good crest factor of chirp signals, simpler and less conflicting measures can be taken compared to experiments based on multisine excitations.

A Dynamic gear load constraints
The maximum amplitude of the excitation signal must be limited to a reasonable value. However, due to the good crest factor of chirp signals, a strong excitation is achievable.

B Coulomb friction:
With a strong excitation over the whole experiment, the impact of Coulomb friction around zero velocity becomes secondary. It acts as a low additional damping force.

C Nonlinear deflection dependent stiffness:
A strong excitation over all frequencies naturally leads to frequency dependent spring deflections in the transmission. Because of this, different regions of the stiffness characteristic dominate over the band of excited frequencies. If the stiffness characteristic is deflection dependent, the shape of the resulting FRF estimate is warped.

D Position dependent dynamics:
The position error is low for harmonic excitations even if they are strong.

E Periodic disturbances:
There are no dominating slow constant velocity components in the excitation and the resulting periodic disturbances are negligible.

F Measurement and discretization noise:
The very good signal to noise ratio and the good crest factor of chirp signals make the experiments insensitive to noise.

Remark 2 (Low amplitude chirp excitation superimposed with a constant velocity profile)**.** *Of course, the sweep signal could also be superimposed with a slow constant velocity in order to avoid nonlinear friction. This is not considered in this paper because for low amplitudes, the multisine can play off its advantages i. e. the existing theory about calculating a best linear approximation of the nonlinear system.*

5.3. An Iterative Procedure for the Determination of Closed Loop Excitations

The experiment design based on chirp excitations uses the assumption that a strong excitation of the system can be guaranteed for all time s. t. the disturbing influence of Coulomb friction becomes negligible. Unfortunately, the plant input $\boldsymbol{u}$, which determines the strength of the plant excitation, cannot be excited directly in the usual tracking configuration of the closed loop, see Figure 2. In order to obtain a reasonable excitation in $\boldsymbol{u}$, an iterative procedure is proposed which leads to a frequency dependent amplitude of the reference excitation signal at $\boldsymbol{r}$.

1. A desired excitation at the plant input
$$\boldsymbol{u}^{\mathrm{des}}(t_i) \overset{\mathcal{F}}{\underset{n_f}{\longmapsto}} \boldsymbol{U}^{\mathrm{des}}(\omega_k) \tag{17}$$
is designed.
2. An initial excitation for the closed loop injection at $\boldsymbol{r}$ is designed, e. g. chirp signals of the type (15) with $A(t)$ set to a constant value A. Such an initial excitation is denoted $\boldsymbol{r}_1$. Its amplitudes may be conservatively low in order to avoid damaging to the robot due to extreme loads.
3. From the experiments with the initial excitation, an initial FRF estimate of the transfer path from $\boldsymbol{r}$ to $\boldsymbol{u}$, $\hat{\boldsymbol{P}}_{1,\boldsymbol{r}\to\boldsymbol{u}}$, can be calculated.
4. Assuming $\hat{\boldsymbol{P}}_{1,\boldsymbol{r}\to\boldsymbol{u}}$ is invertible, its inverse may be used to calculate a new excitation $\boldsymbol{r}_2$ for the closed loop injection.
$$\boldsymbol{R}_2(\omega_k) = \hat{\boldsymbol{P}}^{-1}_{1,\boldsymbol{r}\to\boldsymbol{u}}(\omega_k)\boldsymbol{U}^{\mathrm{des}}(\omega_k) \tag{18}$$
$$\boldsymbol{R}_2(\omega_k) \overset{\mathcal{F}}{\underset{n_f}{\longmapsto}} \boldsymbol{r}_2(t_i) \tag{19}$$
5. Steps 3 and 4 are repeated until the resulting $\boldsymbol{u}$ matches $\boldsymbol{u}^{\mathrm{des}}$. Simply replacing the indices $1 \to i$ and $2 \to i+1$ yields a suitable recursion formula.

Since invertibility of $\hat{\boldsymbol{P}}_{i,\boldsymbol{r}\to\boldsymbol{u}}(\omega_k)$ is assumed, $\boldsymbol{r}$ and $\boldsymbol{u}$ must have the same dimension. This is a reasonable assumption for closed loop tracking configurations. Instead of $\boldsymbol{u}$, any other measurable signal with appropriate dimension and invertible transfer function may be assigned. If the initial excitation $\boldsymbol{r}_1$ is much too low, e. g. if the robot is stuck

in friction for all time, the iteration will not work. A reasonable initial excitation must be chosen.

As a side effect, designing an orthogonal excitation at the plant input $\boldsymbol{u}$ also yields an optimal condition number for $\mathbb{U}(\omega_k)$ which is important for (7). Such a well conditioned $\mathbb{U}(\omega_k)$ is not achieved if an orthogonal excitation is inserted as a reference signal $\boldsymbol{r}$ for the controller.

6. An Academic Example System

A simple but realistic single axis flexible joint robot is considered in the following as an illustrative example to compare the properties of the multisine and the chirp excitation signal. The example is used to back up the discussions from the preceding sections. A similar example is used in [7].

6.1. Simulation Setup

The plant dynamics of the example system are ruled by

$$\Delta\dot{q} = \dot{q}_m - \dot{q}_o, \tag{20}$$
$$\ddot{q}_m = 1/J_m(\tau_m - \tilde{\tau}_{f,c}(\dot{q}_m) - \tau_s(\Delta q) - d(\dot{q}_m - \dot{q}_o)), \tag{21}$$
$$\ddot{q}_o = 1/J_o(\tau_s(\Delta q) + d(\dot{q}_m - \dot{q}_o)), \tag{22}$$

where the used motor inertia and link inertia are $J_m = 35\,\mathrm{kg\,m^2}$ and $J_o = 150\,\mathrm{kg\,m^2}$, respectively. The damping is $d = 400\,\mathrm{N\,m\,s\,rad^{-1}}$ and the Coulomb friction is $F_c \in \{0\,\mathrm{N\,m}, 50\,\mathrm{N\,m}\}$, cf. (1). Finally, the nonlinear stiffness $\tilde{\tau}_{f,c}(\dot{q}_m)$, see (2), is used with the parameters $k_1 = 1.5 \times 10^5\,\mathrm{N\,m\,rad^{-1}}$, $k_2 \in \{k_1, 1.7k_1\}$, and $b = 1 \times 10^{-3}\,\mathrm{rad}$. All initial conditions are set to zero. Note finally that no gravity is considered and consequently there is no static load.

The plant input u is the motor torque τ_m and the measured output y is the motor velocity $\dot{q}_m$. To keep the example simple, the effects are studied in an open loop setting, i. e. the excitation is inserted directly in the input of the plant. Similar results are obtained for closed loop experiments using the iterative procedure proposed in Section 5.3.

There is no noise in the simulation. In order to limit the load of the transmission, the input motor torque τ_m is limited to 150 N m. Depending on the choice of F_c and k_2, the impact of Coulomb friction and nonlinear deflection dependent stiffness on the results of the different experiment designs can be studied. The considered experiment designs are itemized in the following list.

- An odd random phase multisine excitation is designed according to Section 4.2 with $\tilde{f}_l = 1\,\mathrm{Hz}$ and $\tilde{f}_u = 60\,\mathrm{Hz}$. The amplitudes A_s are all chosen equal such that $\max_t |r_{\mathrm{ms}}(t,\phi)| = 150\,\mathrm{N\,m}$ bounds the resulting amplitude. The resulting excitation signal has a duration of 12.3 s. For the averaging, $n_q = 1$ (no noise) and $n_p = 30$. No constant velocity is superimposed.

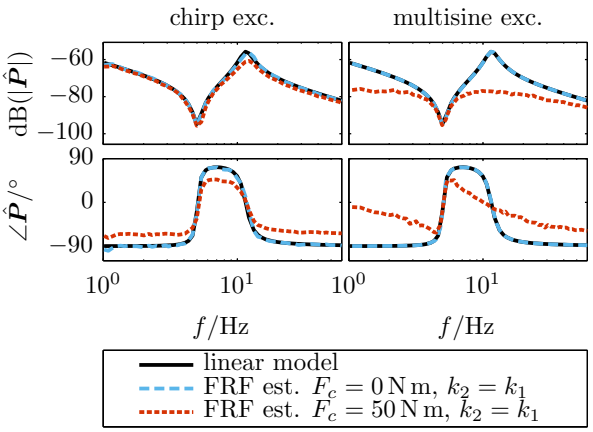

Figure 4: Influence of nonlinear friction on the FRF estimates ($\tau_m \to \dot{q}_m$) of the example system.

- A chirp excitation between $f_l = 1\,\mathrm{Hz}$ and $f_u = 60\,\mathrm{Hz}$ with a duration of 20 s and $A(t) = 150\,\mathrm{N\,m}$.

Depending on the random realization of the multisine, its average power is only about 11 % − 20 % of the average power in the chirp excitation even tough the maximum amplitudes of both signals are bounded by the same threshold.

6.2. Simulation Results

With none of the nonlinearities active, i. e. for the choice $F_c = 0\,\mathrm{N\,m}$ and $k_2 = k_1$, both approaches lead to almost perfect FRF estimates, see Figure 4.

With the choice $F_c = 50\,\mathrm{N\,m}$ and $k_2 = k_1$, the only acting nonlinearity is Coulomb friction. The resulting FRF estimates are depicted in Figure 4. The estimate yielded by the chirp excitation is only slightly perturbed. Since the excitation is strong with an amplitude of 150 N m over all frequencies, the friction acts as an insignificant extra damping force. The main influence can be seen in the phase which is 'pushed together', the resonance and antiresonance show a little less clearly. On the other hand, the resonance peak in the FRF estimate yielded by the multisine excitation is completely concealed because the excitation is too weak. Note that superimposing the multisine with a constant velocity yields the same results like a chirp excitation (not depicted in Figure 4).

With the choice $F_c = 0\,\mathrm{N\,m}$, $k_2 = 1.7k_1$, the only acting nonlinearity is the deflection depending stiffness. Figure 5 depicts the resulting FRF estimates. The FRF estimate yielded by the chirp excitation is warped around the resonance frequency. The nonlinear part of the stiffness characteristic is reached. In the estimate yielded by the multisine excitation, no effect of nonlinear stiffness can be observed since the excitation is too weak. Because of this, the estimate coincides perfectly with the FRF of the linear model. Comparing the two resulting FRF estimates and using the knowledge that higher loads and thus higher

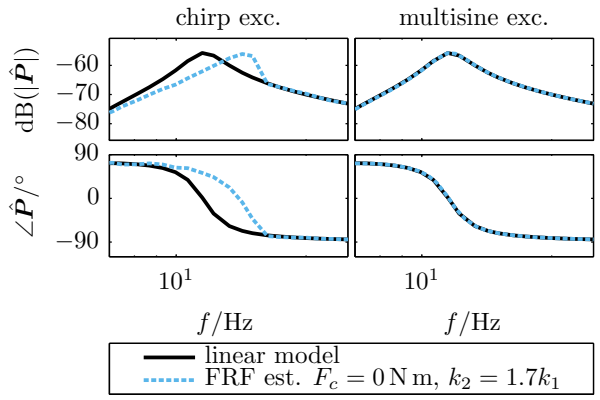

Figure 5: Influence of nonlinear deflection dependent stiffness on the FRF estimates ($\tau_m \to \dot{q}_m$) of the example system.

spring deflections are reached in the resonance, the fact that the stiffness increases for high deflections can be read from the resulting FRF estimates.

7. Determination of FRF Estimates of an Industrial Robot

The FRF estimates obtained for the base axes of the considered industrial robot are presented and the two experiment designs are compared.

7.1. FRF Estimate Based on Multisine Excitation

In order to avoid the disturbing influence of Coulomb friction, the multisine excitations are superimposed with constant velocity profiles $\dot{q}_m^{\mathrm{ref},c}$. The constant velocity profiles are chosen s. t. the maximum position deviation is about $\pm 4°$. The superimposed multisine excitation is designed according to Section 4.2 with $\tilde{f}_l = 2\,\mathrm{Hz}$ and $\tilde{f}_u = 60\,\mathrm{Hz}$. The amplitudes A_s are all chosen equal such that the resulting amplitude is limited to $\max_t |r_{\mathrm{ms}}(t,\phi)| = 0.75\dot{q}_m^{\mathrm{ref},c}$ in order to avoid the zero velocity regime. One realization of the resulting multisine excitation is depicted in Figure 6. The maximum values of the resulting excitation in the input of the plant, i. e. the resulting motor torques are

$$\max|\tau_{m,1}| \approx 200\,\mathrm{N\,m}, \tag{23}$$
$$\max|\tau_{m,2}| \approx 136\,\mathrm{N\,m}, \tag{24}$$
$$\max|\tau_{m,3}| \approx 62\,\mathrm{N\,m}. \tag{25}$$

For the averaging, the experiment is repeated with $n_p = 10$ and $n_q = 5$. Due to the superimposed constant velocity, the effects of nonlinear friction are avoided but periodic disturbances from the motors lead to strong distortions in the FRF estimate, see Figure 8. With a compensation of these deterministic periodic disturbances as proposed in Item 5, the resulting FRF estimate is no longer distorted at the corresponding frequencies, see Figure 8.

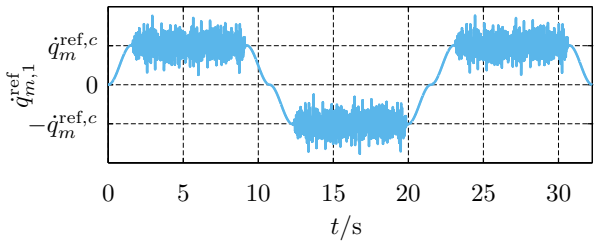

Figure 6: Realization of the odd random multisine for the MIMO identification of an industrial robot: Reference velocity for axis 1.

7.2. FRF Estimate Based on Chirp Excitation

The desired excitation in the input of the plant, i. e. for the motor torques, are chirps between $f_l = 2\,\mathrm{Hz}$ and $f_u = 60\,\mathrm{Hz}$ with a duration of 20 s. The desired amplitudes are chosen frequency dependent as summarized in Table 1.

The initial excitation is inserted as a reference velocity with the amplitudes $A(t) = 0.006\,\mathrm{rad\,s^{-1}}$ for axis 1 & 2 and an amplitude $A(t) = 0.012\,\mathrm{rad\,s^{-1}}$ for axis 3. This corresponds to a very low excitation and the resulting initial FRF estimate is completely distorted as can be seen in Figure 9. The procedure from Section 5.3 is applied to arrive at the desired excitation in the input of the plant.

The axis 3 motor torque which is achieved after six iterations is depicted in Figure 7. It is very closed to the desired $\tau_{m,3}^{\mathrm{des}}$ which is 120 N m at low frequencies and 60 N m at high frequencies, see Table 1. The power spectral density over time of the signal is given in Figure 3. It allows to detect the notable impact of the higher harmonics of the input signal which are present due to the nonlinearities of the system.[7] The resulting FRF estimate after six iterations is depicted in Figure 9.

Experiments show that an orthogonal excitation, as introduced in Section 4 in the context of multisine excitations, is not the best choice for chirp excitation signals. It is advantageous to only change the phase of one input at a time e. g. by using (9) replacing $\phi_{l,k}$ by

$$\tilde{\phi}_{l,k} = \begin{cases} 0 \text{ for } l \neq k \text{ and } l = 1, \\ \pi \text{ for } l = k \text{ and } l > 1. \end{cases} \tag{26}$$

[7] The reader is reminded that these higher harmonics are considered by the procedure proposed for the signal preprocessing.

Table 1: Frequency dependent amplitude for the desired motor torques.

axis	low freq. amplitude	amplitude above 40 Hz
$\tau_{m,1}^{\mathrm{des}}$	100 N m	50 N m
$\tau_{m,2}^{\mathrm{des}}$	150 N m	75 N m
$\tau_{m,3}^{\mathrm{des}}$	120 N m	60 N m

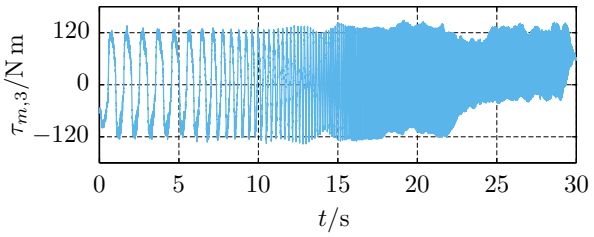

Figure 7: Exemplary axis 3 motor torque resulting from one of the two chirp signals per axis used in the MIMO identification of an industrial robot. Final (6^{th}) iteration.

This can be seen by comparing the channel $\tau_{m,2} \to \dot{q}_{m,1}$ of the FRF estimates resulting from the orthogonal excitation and the excitation defined by (26). Both are depicted in Figure 9. According to physical considerations, the FRF estimate of the channel $\tau_{m,1} \to \dot{q}_{m,2}$ should equal that of the channel $\tau_{m,2} \to \dot{q}_{m,1}$. In the channel $\tau_{m,1} \to \dot{q}_{m,2}$, the peaks of the two FRF estimates are marked and these values are copied to the channel $\tau_{m,2} \to \dot{q}_{m,1}$. Obviously, the correspondence is better for the excitation defined by (26) whose peaks are marked with black circles. For the orthogonal excitation which is marked by red crosses, the difference is at about 10 dB. The reason why the excitation defined by (26) leads to better results is not fully understood. It is assumed that transient effects are responsible.

7.3. Comparison of the Resulting FRF Estimates

In Figure 10, the FRF estimates obtained from the multisine and chirp experiments are compared. As expected, the resonance and antiresonance in the chirp FRF estimate show a little less clearly since the zero velocity regime is not avoided. The resonance peaks of the chirp FRF estimate are not warped compared to the multisine FRF estimate. The combination of both approaches allows to determine the impact of nonlinear deflection dependent stiffness which is negligible for the considered robot. Due to the need to perform the multisine excitation 10×5 ($n_p \times n_q$) times in order to obtain noise free results, the identification procedure based on multisines takes longer than the procedure based on chirps. The procedure based on chirps only needs 6 iterations to arrive at the desired excitation at the plant input.

8. Conclusion

Applying the iterative procedure for the determination of closed loop excitations, the chirp excitation can rely on its high power at each frequency due to its good crest factor. This allows to decrease the disturbing impact of Coulomb friction without avoiding the low velocity regime. This is attractive because the controllers which are designed based on the identified models have no way of avoiding the zero velocity regime. If nonlinear deflection dependent stiffness

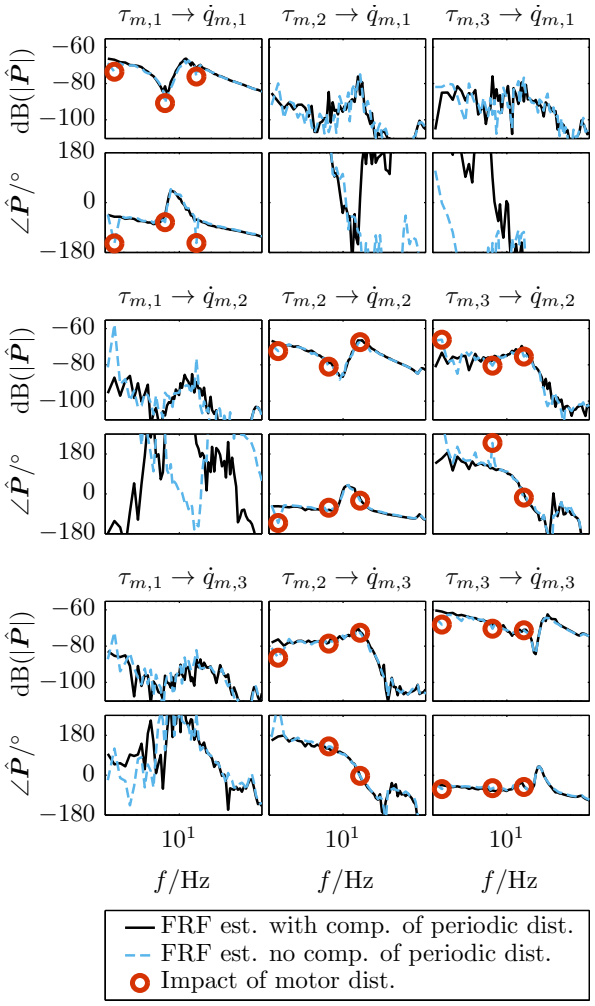

Figure 8: FRF estimates using the multisine excitation with and without compensation of periodic disturbances.

is present, it has an impact on the resulting FRF estimate which is warped. A disadvantage of chirp excitations is the possible damage to the robot caused by high amplitudes of the excitation. The amplitudes must thus be chosen carefully.

A multisine excitation only leads to good results if it is superimposed with a constant velocity in order to avoid Coulomb friction. This severely limits the maximum amplitude of the excitation. The theoretical advantage of multisine excitations, i. e. the fact that it gives a best linear approximation as discussed in Section 4, loses some significance in the face of the severe amplitude limitations in combination with the low crest factor of the excitation. Nonlinear deflection dependent stiffness for example can only be detected with strong excitations. At the same time, a weak excitation has the advantage that the load for the mechanical parts of the robot is low s. t. the determination of FRF estimates for many operating points is unlikely to result in mechanical wear.

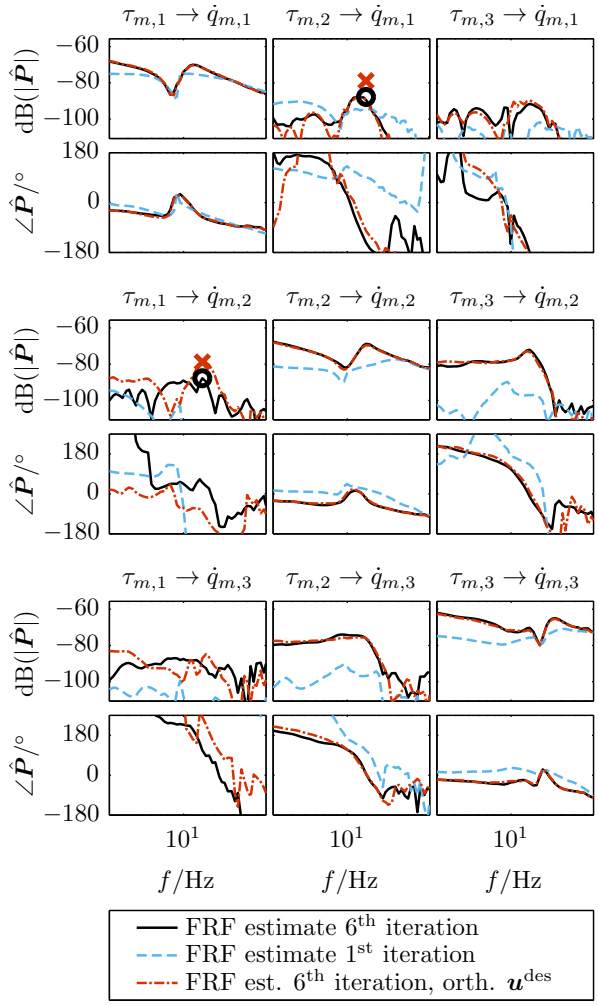

Figure 9: FRF estimates using the chirp excitation for the first and final (6^{th}) iteration.

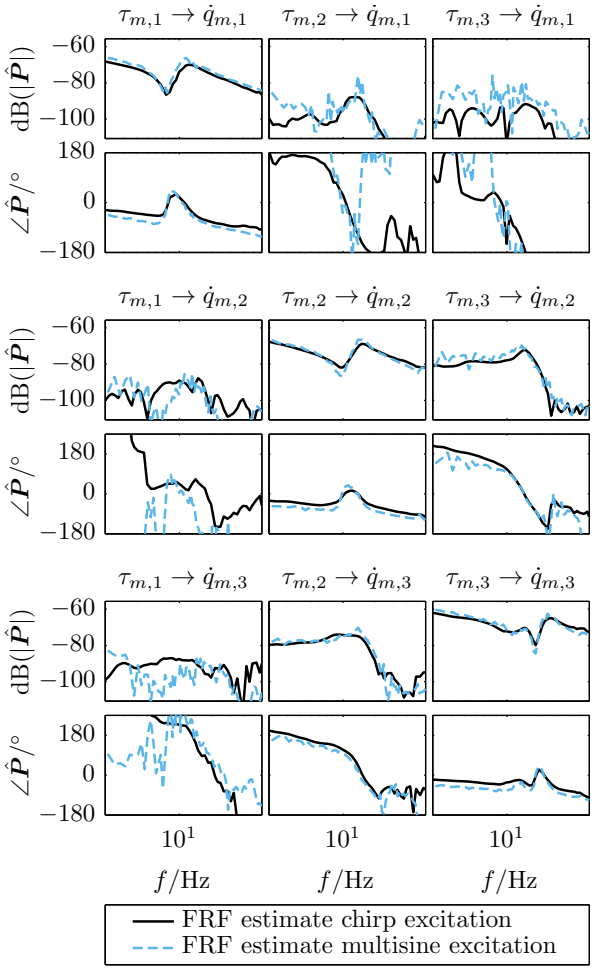

Figure 10: Comparison of FRF estimates resulting from multisine and chirp excitation.

An important synergy of the two approaches is that their combination allows to determine the impact of non-linear stiffness.

[1] E. Berglund and G.E. Hovland. Automatic elasticity tuning of industrial robot manipulators. In *IEEE Conference on Decision and Control*, volume 5, pages 5091–5096, 2000.

[2] L. Ljung. *System Identification: Theory for the User*. PTR Prentice Hall Information and System Sciences Series, 2007.

[3] Matthias Löhning. *Robust Control of Elastic Robots*. PhD thesis, Technischen Universität Hamburg-Harburg, 2011.

[4] S. Maier, M. Bodson, and J. Bals. Periodic disturbance rejection of a PMSM with adaptive control algorithms. In *IEEE International Electric Machines and Drives Conference*, 2011.

[5] M. Östring, S. Gunnarsson, and M. Norrlöf. Closed-loop identification of an industrial robot containing flexibilities. *Control Engineering Practise*, 11:291–300, 2003.

[6] J. Schoukens, R. Pintelon, T. Dobrowiecki, and Y. Rolain. Identification of linear systems with nonlinear distortions. *Automatica*, 41(3):491–504, 2005.

[7] E. Wernholt. *Multivariable Frequency-Domain Identification of Industrial Robots*. Linköping studies in science and technology. dissertations. no. 1138, Department of Electrical Engineering Linköping University, SE-581 83 Linköping, Sweden, November 2007.

[8] E. Wernholt and S. Gunnarsson. Estimation of nonlinear effects in frequency domain identification of industrial robots. *IEEE Transactions on Instrumentation and Measurement*, 57(4):856–863, 2008.

[9] Erik Wernholt and Stig Moberg. Experimental comparison of methods for multivariable frequency response function estimation. In *17th IFAC World Congress*, 2007.